Langmuir

Article

pubs.acs.org/Langmuir

Fuzzy Nanoassembly of Polyelectrolyte and Layered Clay Multicomposite toward a Reliable Gas Barrier

Jin Hwan Choi, Young Wook Park, Tae Hyun Park, Eun Ho Song, Hyun Jun Lee, Hakkoo Kim, Se Joong Shin, Vincent Lau Chun Fai, and Byeong-Kwon Ju*

Display and Nanosystem Laboratory, College of Engineering, Korea University, 5-1, Anam-Dong, Seongbuk-Gu, Seoul 136-701, Republic of Korea

Supporting Information

ABSTRACT: Flexible and transparent gas-diffusion barriers have played an important role in recent years. The present study describes a flexible barrier film with a tailored architecture of cationic polyelectrolytes and clay/polymer nanoassemblies. Highly oriented and well-aligned barrier films were achieved by the consecutive absorption of flexible cationic polymer and anionic montmorillonite platelets. The experimental results showed that the layer-by-layer deposition of oppositely charged thin films containing self-assembled poly(vinyl alcohol) and montmorillonites improved their gas barrier characteristics based on the Ca degradation test, enhancing their optical transparency. This nanostructure, fabricated using a solution process, is useful in many applications, for example, flexible and moisture-free organic electronics. This simple and fast method is suitable for the mass coating of large surface areas, as required in industry.

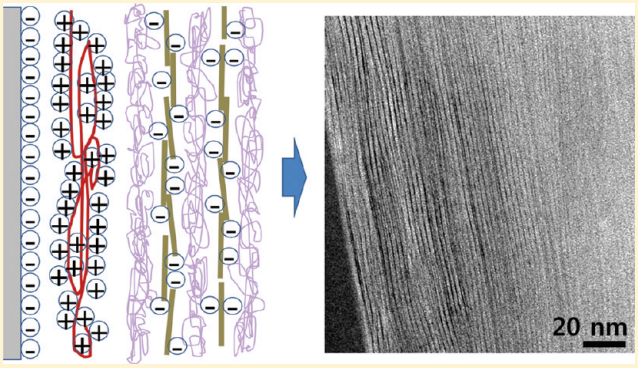

INTRODUCTION

Significant developments and breakthroughs in the electronics industry have enabled the production of thinner, lighter, and more flexible devices. However, the environmental stability and reliability of flexible devices are still a major concern.[1−5] It is widely known that polymeric devices are highly susceptible to permeation by water and oxygen.[1−4] Many groups have therefore conducted research into the films produced using alumina-, and silica-based materials for moisture-diffusion barrier applications. These materials can be deposited by various physical and chemical techniques, such as evaporation, oxidation, chemical vapor deposition, plasma polymerization, and nanocomposition.[1−4] For example, Carcia et al.[4] showed that films fabricated by atomic-layer deposition have high barrier efficiencies. However, inorganic materials are notorious for cracking and having pinhole defects in the layer surface when bent.[6] Weaver et al.[2] proposed organic/inorganic multibarrier stacks with ultralow gas permeation rates. However, these organic/inorganic thin films suffer from low productivity and high-cost fabrication processes. Conceptually, new methodologies are therefore needed.

Nanoparticle-based solution processes for the fabrication of thin-film barriers have been proposed in recent years.[7−10] This concept uses disk-shaped inorganic montmorillonite (MTM) with polymeric materials to produce hard/soft structures.[11−18] The individual clay flakes consist of approximately 1 nm thick plate-shaped nanoparticles, with an aspect ratio of 100−1000.[17] MTM has a cationic exchange capacity of 0.926 meq/g and a negative surface charge in deionized (DI) water.[18] The key factor for the use of nanoclay in barrier layers is its alignment parallel to substrates.[14−16,18] As shown in Figure 1a, a well-aligned clay mineral in a polymer matrix can extend the diffusion path of water molecules and may be able to enhance the barrier properties. Therefore, the ability to incorporate clay into a polymeric matrix with a high level of exfoliation and orientation is one of the most important challenges in the fabrication of polymer−clay nanocomposites with enhanced barrier performances. Opacity and irregular platelet alignment ultimately impair the barrier characteristics. MTMs are inorganic (SiO_2) nanoparticles. Water vapor therefore cannot penetrate the clay platelets. As shown in Figure 1a, the diffusion path length of the water vapor can be increased by layered clay, if the clay platelets lie parallel to the substrates, because clay platelets have high aspect ratios. Without the layered clay, the film containing polymer layers cannot show gas barrier characteristics because water vapors easily pass through the organic materials.

In this paper, we introduce a simple and rapid methodology for the fabrication of large-area, lightweight barrier films. We explored concepts that enable self-assembled single-step layer growth. A self-aligned clay multilayer can be fabricated by the absorption of poly(vinyl alcohol) (PVA) onto MTM because of

Received: December 7, 2011
Revised: March 31, 2012
Published: April 6, 2012

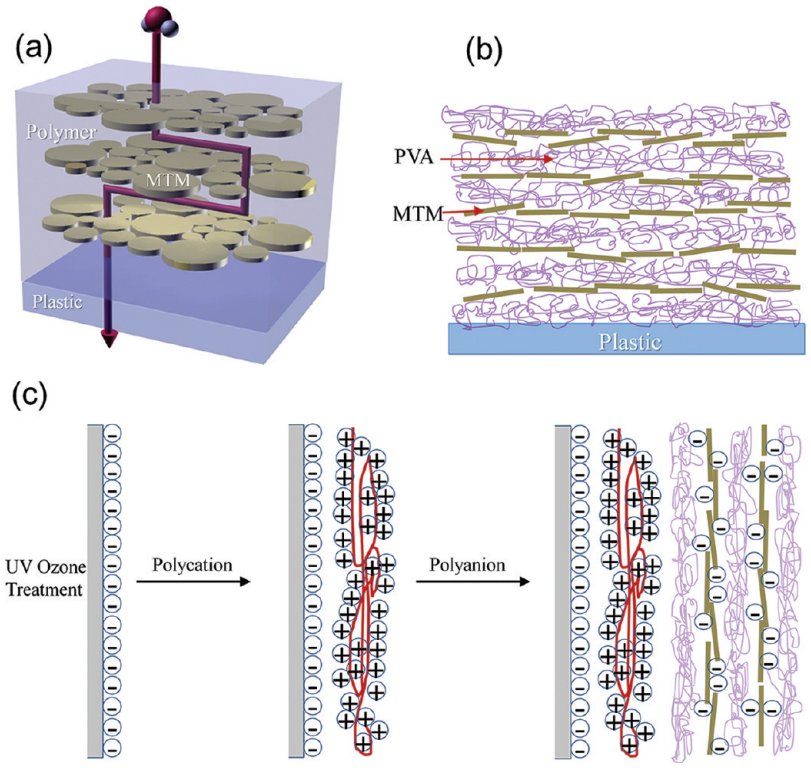

Figure 1. (a) Schematic representation of the roundabout path that water molecules must take through the nanoclay-filled polymer. (b) Schematic diagram of the one-step nanocomposite of MTM/PVA. Because of its strong adhesion force and hydrogen bonding, PVA can be easily intercalated in the MTM platelets. (c) Simplified molecular image of the first two deposition steps, depicting film absorption initiated by the negatively charged PES surface, followed by the formation of the cationic polymer and anionic MTM/PVA multicomposite.

their absorption capabilities and strong hydrogen bonding,[14,15] as schematically shown in Figure 1b. A thin and transparent gas barrier can be made by the electrostatic assembly of a cationic polymer and the MTM/PVA multicomposite. In this case, strong electrostatic attraction occurs between a charged surface and oppositely charged molecule in solution.[18−20] These films are homogeneous monolayers arising from submonolayer coverage after the first deposition cycle and subsequent completion of the surface coverage. The cyclic repetition of both absorption steps leads to the formation of multilayer structures.

The process, which is extremely simple, is depicted in Figure 1c for the case of deposition of a cationic polymer and an anionic MTM/PVA composite. These steps represent the absorption of a polyanion and polycation and are the basic buildup sequence for the simplest film architecture, $(A/B/C/B)_n$. The counterions are omitted for clarity. MTM/PVA multilayers can be used to prepare the preparation building-block structures based on simple, scalable processing methods. This approach, which enables self-control of the molecular orientation and nanoscale organization, results in good gas barrier performance with high light transmission.

EXPERIMENTAL SECTION

Materials. Anionic MTM (Cloisite Na^+) was purchased from Southern Clay Products. This is negatively charged in DI water, and each platelet has a diameter of 100−1000 nm and a thickness of about 1 nm.[17] PVA (M_n = 30 000−70 000, 87−90% hydrolyzed), glutaraldehyde (25 wt % in water), and poly(ethyleneimide) solution (PEI, M_n = 1200, 50 wt % in water) were purchased from Sigma-Aldrich. Poly(methyl acrylic acid) solution (PMA, M_w = 4000−6000, 40 wt % in water) was purchased from Fluka (part of Sigma-Aldrich). The water used for all solutions was 18 MΩ DI Milli-Q water.

Method. Self-assembled MTM/PVA films were fabricated using the following process. A solution of 0.5 wt % MTM in DI water and 0.5 wt % aqueous PVA in DI water were prepared by magnetic stirring for 24 h at 20 °C. The MTM solution (pH 6) was poured into the PVA dispersion (pH 4) and stirred for 3 h to allow for fine absorption of the polymer onto the clay platelets. Before an air-gun spraying process, glutaraldehyde was added to the MTM/PVA slurry (pH 7) as a cross-linking agent. Poly(ethersulfone) (PES, 100 μm, fabricated by Cheil Industry, Inc., Republic of Korea) substrates were cleaned by immersion in ethanol for 30 min, followed by thorough sonication, and rinsing with DI water. The MTM/PVA slurry with glutaraldehyde was sprayed onto the cleaned PES substrates for a few seconds, and the resulting film on PES was dried at 80 °C for 30 min.

Layer-by-layer (LbL) deposition[19] of cationic polymers, anionic polymers, and anionic MTM solutions was performed using the following process. Aqueous dispersions of PEI (0.5 wt % in DI water) and PMA (0.5 wt % in DI water) were prepared by magnetic stirring for 24 h at 20 °C. The cleaned PES substrate was treated with ultraviolet (UV) ozone for 20 min to generate OH^- radicals on its surface. The anionic-treated substrate was dipped in cationic PEI aqueous solution (pH 10) for 3 min, followed by DI water rinsing and air drying. The same procedure was performed for the subsequent layers of anionic PMA (pH 8), cationic PEI, and anionic MTM aqueous solutions. After the initial layers were depositied, the plastic sample was dipped and removed immediately from the same solutions.

The LbL assembly of cationic and anionic polymers with a self-assembled MTM/PVA film was carried out using the following process. The procedure begins with the preparation of PVA-coated MTM platelets in water. The undissolved MTM in the PVA solution can be removed by an *in situ* sedimentation process by adding a cross-linking agent, such as glutaraldehyde, to the slurry. After the cleaning of the PES film, UV ozone treatment, and cationic PEI, anionic PMA, and PEI dipping procedures, the film with a cationic surface charge was

dx.doi.org/10.1021/la300831p | *Langmuir* 2012, 28, 6826−6831

dipped in a MTM/PVA mixture solution, followed by gentle removal and drying at 80 °C for 1 min. The above procedure was repeated several times as necessary. The thickness and light transmission values can be varied by changing the weight percentages of the aqueous solutions, the surface charge of the electrolyte, and the number of times the LbL processes are repeated.

Ca Degradation Test. The moisture barrier properties were characterized by measurements of the water vapor transmission rates (WVTRs, g m^{-2} day^{-1}). The Ca test based on electrical measurements of Ca degradation has previously been reported.[21,22] The amount of oxidative degradation in a thin Ca sensor is monitored by resistance measurements. The water vapor, permeating through the gas barrier on the PES, oxidizes the Ca. This is reflected by the decrease in the current when a constant voltage (5 mV) is applied and is monitored using a two-point probe system.

Analysis Using Transmission Electron Microscopy (TEM) and UV−Vis Spectrometry. The focused ion beam technique (FIB, NOVA 600 Nanolab) was used to prepare cross-sectional specimens of the barrier films deposited on a Si wafer for TEM analysis. Before deposition of a thin Pt layer on the films to enhance heat and charge transfer, an acrylate resin layer was coated on the films to protect them against damage from the electron beam during Pt deposition. A lift-out technique, consisting of a milling process to form a stair-step trench in the film area, polishing, and edge-cutting steps, was used. The specimens, which were suitable for high-resolution imaging, were then transferred to the TEM grid. The TEM observations were performed using a Tecnai 20 instrument operated at 200 kV to enhance the contrast between the clay and polymer layers. TEM detects the electrons in a fluorescent plate after the accelerated electrons have passed through the films. The optical transmittance values of the barrier films were measured using a UV−vis spectrometer (OPTIZEN 3220UV, Mecasys) by determining the transmission of UV−vis light through the films. The UV−vis spectrometer exposed a barrier film to the UV and visible regions of the electromagnetic spectrum when the film was placed in a UV−vis beam. The amount of light that was not absorbed and therefore passed through the film to the detector depended upon the type of film. The UV−vis spectrometer was adjusted so that the wavelength of the emitted light was in the range of 300−800 nm. The bare PES coated with a clay barrier layer was cleaned because dust might affect the amount of UV light reaching the detector in the UV−vis spectrometer.

RESULTS AND DISCUSSION

For the first reference sample, a MTM/PVA mixture with a glutaraldehyde cross-linking agent was sprayed onto a PES substrate. The high-resolution TEM (HRTEM) images in Figure 2 show a well-spaced composite film. The orientation of the assembly is assisted by the self-ordering of the high-aspect-ratio nanoclays, good absorption capabilities, significant PVA hydrogen bonding, and glutaraldehyde cross-linking.[14,15] The film containing MTM/PVA consisted of nanoclay layers with a thickness of about 1 nm and PVA layers with a thickness of about 2−3 nm. The total thickness of the sprayed MTM/PVA film was about 1 μm. The thicknesses of the PVA layers can be changed by varying the solution dispersion, but the thicknesses of the clay layers cannot be changed (1 nm thick and 100−1000 nm in diameter). Additional mixing time did not assist the alignment of MTM in PVA even after 1 week of stirring. However, several misaligned positions were found, and these will impair the barrier characteristics and lead to opacity (see the Supporting Information). Fine alignment could be achieved using an electrostatic assembly method.

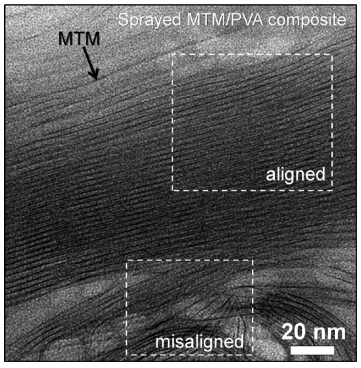

Figure 2. Cross-sectional HRTEM image. The MTM/PVA multicomposite shows a well-spaced layered structure. The black portions indicate clay platelets. Although the film shows strong orientation of the nanoclay platelets parallel to the substrate, the misaligned regions impair the film transparency and barrier properties.

As the second reference film, we fabricated a film by LbL deposition of cationic polymers, anionic polymers, and MTM solutions. PEI was used as the cationic polymer, and PMA was used as the anionic polymer. DI water was used for all aqueous solutions. LbL deposition is a method of laminating functional thin films through alternating exposure of a substrate to aqueous anionic and cationic solutions.[18−20] As shown in Figure 3, the fabricated film has a nanoarchitecture with good positioning of the individual layers. The electrostatic attraction between the oppositely charged films can assist in nanoscale multilayer buildup.[19] This architecture has an overall thickness of approximately 50 nm after five cycles of the LbL process. Figure 3 shows the high level of orientation of the nanoassembly, with flakes and polyelectrolytes lying parallel to the PES substrates. This near-perfect orientation is made possible by the LbL process.[18] However, despite the good orientation and high transparency, the LbL process has the limitation that numerous dipping processes are required to form a multilayer, in contrast to the case for MTM/PVA self-aligned multicomposites.

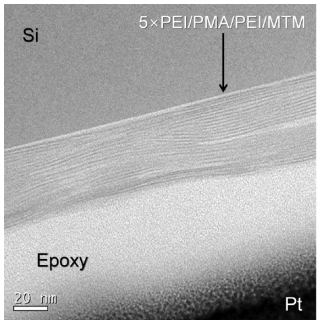

Figure 3. TEM image of the five-cycle LbL film showing the near-perfectly oriented and aligned clay and polymers. Each layer has a thickness of about 1 nm, and the overall thickness of the film is approximately 50 nm. This explains its high transparency.

For the fabrication of a reliable gas barrier film, as shown in Figure 1c, we exposed the PEI/PMA/PEI-coated PES to a MTM/PVA slurry for additional self-growth of the organic/inorganic multicomposite. The cross-sectional TEM images in Figure 4a of the three-cycle LbL of PEI/PMA/PEI/(MTM/PVA) coated on a 100 nm PES film show highly ordered clay platelets with automatically generated MTM/PVA multilayers. Each polymer molecule connects two or more nanoclay platelets (the black lines in the TEM images indicate the clay platelets), and the total thickness of the barrier film was about

dx.doi.org/10.1021/la300831p | Langmuir 2012, 28, 6826−6831

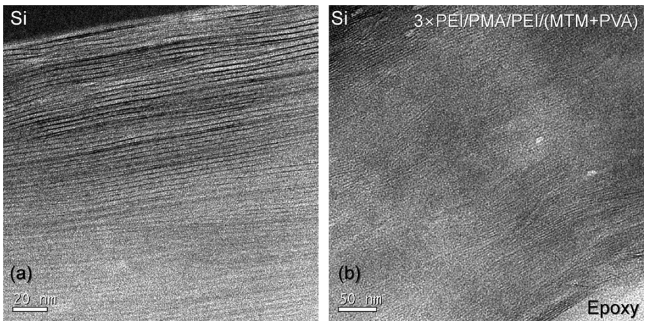

Figure 4. TEM images of three cycles of layered cationic PEI, anionic PMA, PEI, and anionic MTM/PVA multi-assembly. These images confirm that numerous hard/soft layers were generated with high orientation parallel to the substrate. The thickness of each layer is 2−3 nm, and the total thickness of the barrier film is approximately 500 nm. Scale bars = (a) 20 nm and (b) 50 nm.

500 nm according to Figure 4b. LbL clay/polymer multilayer films characteristically show strong stratification and a high degree of layered order. Also, the absorption of PVA onto MTM by both covalent bonds and physical absorption leads to the formation of alternating laminate barrier films with a thickness of approximately 2 nm. Coupling LbL deposition by electrostatic interactions between oppositely charged thin films with the strong self-assembling tendency of MTM/PVA causes the permeating molecules to travel along much longer diffusion channels between the PEI, PMA, and PEI nanoassemblies and also between MTM and PVA spaces. This method allows for simple step layer growth in a self-assembled manner, and a hard/soft composite is obtained using a low-cost, simple, rapid, and scalable method. Information on the thickness variations of the deposition cycles was shown in Figure 5.

With respect to the film coating, the light transmission is of major importance. The optical properties of the fabricated films were characterized by UV−vis spectroscopy. UV−vis spectroscopy reveals that MTM/PVA sprayed on the PES substrate as a reference has a transmission value of less than 80%. This is caused by misaligned regions, which form high-density clay masses and induce undesireble roughness in the film (see the Supporting Information). Usually, LbL films have a high level of transparency.[18−20] The PEI/PMA/PEI/MTM (as shown in the Supporting Information), and PEI/PMA/PEI/(MTM/PVA) LbL films have an average light transmission greater than 85% throughout the visible spectrum (350−750 nm), as shown in Figure 6. These high transparencies were the result of high concentrations of well-oriented nanoclays. As seen in the inset of Figure 6, the three-cycle LbL PEI/PMA/PEI/(MTM/PVA) film is not blurred and the background picture is clearly visible. This result indicates that the process described in this paper enables the formation of uniform and well-ordered nanostructured films that can be applied to optical devices.

The gas-diffusion barrier properties were characterized using WVTR measurements. A Ca test for evaluation of WVTRs using electrical measurements of Ca oxidation has previously been reported.[21,22] A schematic diagram of the Ca test is shown in Figure 7a. Using this test cell, we can derive the permeation rate by measuring the Ca conductance curve when Ca is oxidized as a result of water permeation through the barrier film on a plastic substrate. We can calculate the WVTR from

$$\mathrm{WVTR} = \delta \frac{2M[\mathrm{H_2O}]}{M[\mathrm{Ca}]}\left(1 - \frac{R_i}{R}\right)h_i \frac{24\ \mathrm{h}}{t} \qquad (1)$$

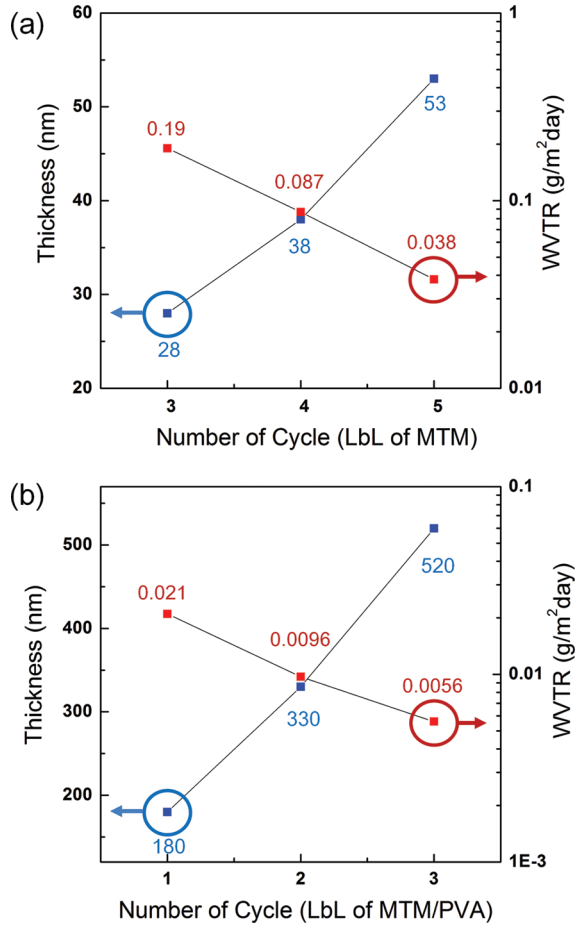

Figure 5. Layer thickness versus deposition cycles and information on WVTRs versus layer number of (a) PEI/PMA/PEI/MTM and (b) PEI/PMA/PEI/(MTM/PVA).

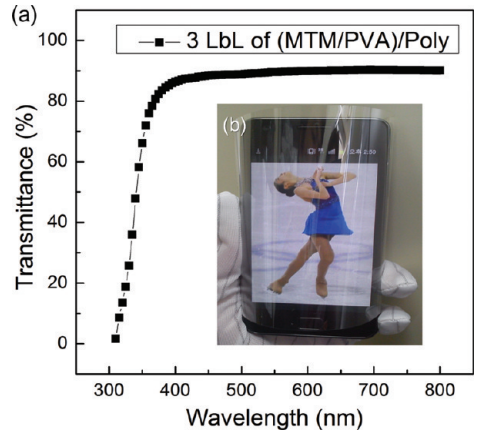

Figure 6. (a) Light transmission curves of the three-cycle LbL of PEI/PMA/PEI/(MTM/PVA) coated on a 100 nm PES film (Figure 4 shows the HRTEM image of this) and (b) photographs of this flexible barrier film. The light transmissions of the other reference films are shown in the Supporting Information.

where h denotes the Ca height, R is the resistance of the Ca sensor connected to silver electrodes, δ is the Ca density, and M is the molar mass of the indicated reagent. R_i and h_i are the initial values of R and h. The WVTR is derived from the conductance, which is indicated by a decrease in the Ca height Δh versus the elapsed time Δt.[21,22]

dx.doi.org/10.1021/la300831p | Langmuir 2012, 28, 6826−6831

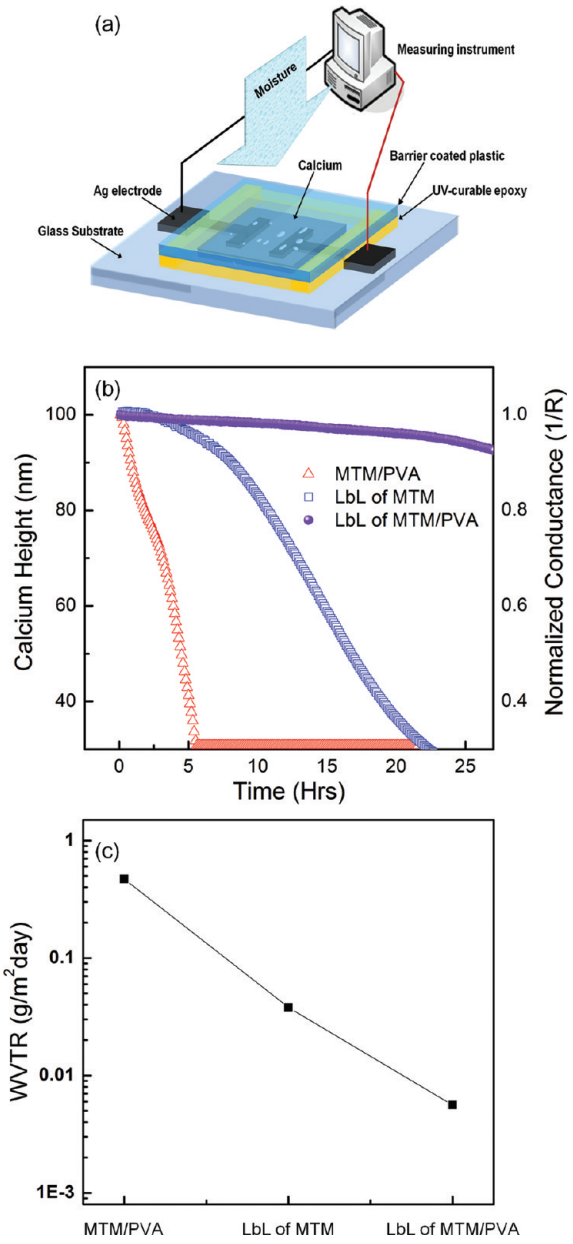

Figure 7. (a) Structure of the Ca test cell. If the water molecules permeating through the barrier film on the plastic substrate react with Ca, then the electrical resistance of the thin Ca changes. (b) Ca degradation curve versus elapsed time through the sprayed MTM/PVA multicomposite with the glutaraldehyde cross-linking agent, five-cycle LbL PEI/PMA/PEI/MTM ultrathin barrier film, and three-cycle LbL PEI/PMA/PEI/(MTM/PVA) multi-assembly at 20 °C and 60% RH. (c) WVTR for each manufacturing process.

The diffusion paths of water molecules (see Figure 1a) in the nanolayered films can be predicted as follows. In this multistructure, the diameters of the inorganic clay platelets in the polymer matrix are so long in comparison to their thicknesses that the gas-diffusion vector is almost parallel to the plane of each layer, thereby extending the diffusion path.[23,24] For a clay of physical thickness t and spacing between organic regions and clay platelets s, where $s \gg t$, the diffusion path (P) in the multilayer is approximately

$$P = t_1 + s_1 + t_2 + s_2 + ... + t_n + s_n \approx ns \quad (2)$$

as shown schematically in Figure 1a.

The WVTRs of these films were evaluated using the Ca test (Figure 7a). The permeation curves at 20 °C and 60% relative humidity (RH) of a nanoassembled MTM/PVA thick and opaque film, a PEI/PMA/PEI/MTM-layered film formed by five LBL cycles, and a PEI/PMA/PEI/(cross-linked MTM/PVA) film formed by three LBL cycles are presented in Figure 7b. In comparison to that of bare PES (1.38 g m^{-2} day^{-1}), the WVTR of the sprayed MTM/PVA assemblies on the PES substrate shows a lower permeation value of 4.7×10^{-1} g m^{-2} day^{-1} according to the Ca degradation curves versus elapsed time. This relatively poor barrier performance, which is attributed to misaligned regions, can provide gas molecules with diffusion paths even when regions with a high level of clay orientation exist. This one-step mixture and deposition procedure cannot achieve high transparency and good barrier performance because it produces irregular alignments.

Near-perfect orientation and alignment between the clay and polymer were possible with the LbL process. The use of polyelectrolytes is advantageous because good adhesion between the organic layers and underlying surfaces requires ionic bonds. The WVTR of the five-cycle LbL PEI/PMA/PEI/MTM film was measured under the same environmental conditions as shown in Figure 7b. A WVTR of 3.8×10^{-2} g m^{-2} day^{-1} was calculated, using the water permeation equation. Highly aligned nanoparticles with disk-filled polymers have been shown to exhibit enhanced barrier properties with high light transmission because of the high-aspect-ratio platelets causing the gas molecules to travel along an extensive diffusion path. This barrier performance is also believed to be achieved because the primary amine groups of PEI and the carboxylic acid groups of PMA are ideal for cross-linking.[18] However, although this barrier film has high transparency (almost the same value as that of the bare PES film in the visible region; see the Supporting Information) and a relatively low permeation rate, tedious processes (dipping, rinsing, and drying) are required to improve the impermeability of the barrier.

As shown in Figure 7b, the MTM/PVA composite with PEI and PMA electrostatic adhesive layers and an overall thickness of approximately 500 nm showed a WVTR value of 5.6×10^{-3} g m^{-2} day^{-1} at 20 °C and 60% RH. In comparison to previous results, such as 9.3×10^{-2} g m^{-2} day^{-1} at 100% RH for 7 quadlayers reported by Grunlan and co-workers[18] and 20 bilayers reported by Kang et al.,[25] our results showed higher barrier properties with a lower number of deposition cycles. Our results are the best reported thus far for gas permeation performance using a non-vacuum process under the above environmental conditions. The WVTRs of the films decreased rapidly, depending upon the manufacturing process, as shown in Figure 7c. Bare MTM has an ionic energy similar to those of PEI and PMA. DI water has an electrical resistance of about 18 MΩ. The resistances of the solutions of MTM, PEI, and PMA were about 35, 20, and 18 KΩ. The electrical resistance of the MTM/PVA solution was about 37 KΩ; therefore, PVA aggregated to MTM could not seriously affect the ionic properties of MTM/PVA solution, and MTM/PVA had a negative charge similar to that of the MTM solution.

These results confirm that well-oriented clay/polymer assemblies and the good absorption properties of PVA significantly extended the gas-diffusion path. In contrast to LbL layers (deposited one layer at a time), this film incorporates numerous separate layer (as shown in Figure 4) by self-assembly of PVA onto MTM and also allows the clay platelets to orient themselves with the largest dimension

dx.doi.org/10.1021/la300831p | Langmuir 2012, 28, 6826−6831

parallel to the surface through electrostatic forces; the resulting films show high light transmission characteristics. Although these nanoparticles provide a route for diffusion of water molecules through the gaps between the platelets, the hard/soft structure could effectively decrease the gas permeation rate.

CONCLUSION

The developed films are promising for a wide variety of applications, including flexible organic electronics, because of their flexibility, transparency, and gas-shielding properties. The experimental results showed that the LbL deposition of oppositely charged thin films containing self-assembled PVA and MTMs improved the barrier characteristics, with well-aligned hard/soft multilayers. This method led to the formation of a simple and dynamic structure that provided a well-aligned and self-assembled thin-film barrier. This LbL assembly of polyelectrolytes with MTM/PVA nanocomposites will be useful for many applications. This simple and fast method is suitable for the mass coating of large areas, and the resulting films have reliable gas-barrier performances and high light transmission.

ASSOCIATED CONTENT

Supporting Information

Additional HRTEM, atomic force microscopy phase, and light transmission curves of the polymer/nanoclay multicomposites (Figures S1−S7). This material is available free of charge via the Internet at http://pubs.acs.org.

AUTHOR INFORMATION

Corresponding Author

*Telephone: +82-(0)2-3290-3671. Fax: +82-(0)2-3290-3791. E-mail: bkju@korea.ac.kr.

Notes

The authors declare no competing financial interest.

ACKNOWLEDGMENTS

This work was supported by the RFID R&D Program of MKE/KEIT (10035225, Development of Core Technology for High Performance AMOLED on Plastic), a Grant-in-Aid (10030041) under the Next-Generation New Technology Development Programs from the Ministry of Knowledge Economy of the Korean government, and the Basic Science Research Program through the National Research Foundation of Korea (NRF) funded by the Ministry of Education, Science and Technology (2009-0083126). The authors thank the staff of KBSI for technical assistance.

REFERENCES

(1) Chwang, A. B.; Rothman, M. A.; Mao, S. Y.; Hewitt, R. H.; Weaver, M. S.; Silvernail, J. A.; Rajan, K.; Hack, M.; Brown, J. J.; Chu, X.; Moro, L.; Krajewski, T.; Rutherford, N. Thin film encapsulated flexible organic electroluminescent displays. *Appl. Phys. Lett.* **2003**, *83*, 413.

(2) Weaver, M. S.; Michalski, L. A.; Rajan, K.; Rothman, M. A.; Silvernail, J. A.; Brown, J. J.; Burrows, P. E.; Graff, G. L.; Gross, M. E.; Martin, P. M.; Hall, M.; Mast, E.; Bonham, C.; Bennett, W.; Zumhoff, M. Organic light-emitting devices with extended operating lifetimes on plastic substrates. *Appl. Phys. Lett.* **2002**, *81*, 2929.

(3) Dameron, A. A.; Davidson, S. D.; Burton, B. B.; Carcia, P. F.; Mclean, R. S.; George, S. M. Gas diffusion barriers on polymers using multilayers fabricated by Al_2O_3 and rapid SiO_2 atomic layer deposition. *J. Phys. Chem. C* **2008**, *112*, 4573−4580.

(4) Carcia, P. F.; Mclean, R. S.; Reilly, M. H.; Groner, M. D.; George, S. M. Ca test of Al_2O_3 gas diffusion barriers grown by atomic layer deposition on polymers. *Appl. Phys. Lett.* **2006**, *89*, 031915.

(5) Hauch, J. A.; Schilinsky, P.; Choulis, S. A.; Rajoelson, S.; Brabec, C. The impact of water vapor transmission rate on the lifetime of flexible polymer solar cells. *J. Appl. Phys.* **2008**, *93*, 103306.

(6) Choi, J.; Kim, Y.; Park, Y.; Park, T.; Jeong, J.; Choi, H.; Song, E.; Lee, J.; Kim, C.; Ju, B. Highly conformal SiO_2/Al_2O_3 nanolaminate gas-diffusion barriers for large-area flexible electronics applications. *Nanotechnology* **2010**, *21*, 475203.

(7) Moller, M. W.; Lunkenbein, T.; Kalo, H.; Schieder, M.; Kunz, D. A.; Breu, J. Barrier properties of synthetic clay with a kilo-aspect ratio. *Adv. Mater.* **2010**, *22*, 5245−5249.

(8) Grunlan, J. C.; Grigorian, A.; Hamilton, C. B.; Mehrabi, A. R. Effect of clay concentration on the oxygen permeability and optical properties of a modified poly(vinyl alcohol). *J. Appl. Polym. Sci.* **2004**, *93*, 1102−1109.

(9) Triantafyllidis, K. S.; LeBaron, P. C.; Park, I.; Pinnavaia, T. J. Epoxy-clay fabric film composites with unprecedented oxygen-barrier properties. *Chem. Mater.* **2006**, *18*, 4393−4398.

(10) Ebina, T.; Mizukami, F. Flexible transparent clay films with heat-resistant and high gas-barrier properties. *Adv. Mater.* **2007**, *19*, 2450.

(11) Jang, W.; Rawson, I.; Grunlan, J. C. Layer-by-layer assembly of thin film oxygen barrier. *Thin Solid Films* **2008**, *516*, 4819−4825.

(12) Lin, J.; Chu, C.; Chiang, M.; Tsai, W. Manipulating assemblies of high-aspect-ratio clays and fatty amine salts to form surfaces exhibiting a lotus effect. *Adv. Mater.* **2006**, *18*, 3248−3252.

(13) Eckle, M.; Decher, G. Tuning the performance of layer-by-layer assembled organic light emitting diodes by controlling the position of isolating clay barrier sheets. *Nano Lett.* **2001**, *1*, 45−49.

(14) Walther, A.; Bjurhager, I.; Malho, J.; Pere, J.; Ruokolainen, J.; Berglund, L. A.; Ikkala, O. Large-area, lightweight and thick biomimetic composites with superior material properties via fast, economic, and green pathways. *Nano Lett.* **2010**, *10*, 2742−2748.

(15) Podsiadlo, P.; Kaushik, A. K.; Arruda, E. M.; Waas, A. M.; Shim, B. S.; Xu, J.; Nandivada, H.; Pumplin, B. G.; Lahann, J.; Ramamoorthy, A.; Kotov, N. A. Ultrastrong and stiff layered polymer nanocomposites. *Science* **2007**, *318*, 80−83.

(16) Priolo, M. A.; Gamboa, D.; Grunlan, J. C. Transparent clay−polymer nano brick wall assemblies with tailorable oxygen barrier. *Appl. Mater. Interfaces* **2010**, *2*, 313−20.

(17) Ploehn, H. J.; Liu, C. Quantitative analysis of montmorillonite platelet size by atomic force microscopy. *Ind. Eng. Chem. Res.* **2006**, *45*, 7025−7034.

(18) Priolo, M. A.; Gamboa, D.; Holder, K. M.; Grunlan, J. C. Super gas barrier of transparent polymer−clay multilayer ultrathin films. *Nano Lett.* **2010**, *10*, 4970−4974.

(19) Kleinfeld, E. R.; Ferguson, G. S. Fuzzy nanoassemblies: Toward layered polymeric multicomposites. *Science* **1994**, *265*, 370−373.

(20) Decher, G. Fuzzy nanoassemblies: Toward layered polymeric multicomposites. *Science* **1997**, *277*, 1232−1236.

(21) Paetzold, R.; Winnacker, A; Henseler, D.; Cesari, V.; Heuser, K. Permeation rate measurements by electrical analysis of calcium corrosion. *Rev. Sci. Instrum.* **2003**, *74*, 5147−5150.

(22) Choi, J. H.; Kim, Y. M.; Park, Y. W.; Huh, J. W.; Kim, I. S.; Hwang, H. N.; Ju, B. K. Evaluation of gas permeation barrier properties using electrical measurements of calcium degradation. *Rev. Sci. Instrum.* **2007**, *78*, 064701.

(23) Chen, T. N.; Wuu, D. S.; Wu, C. C.; Chiang, C. C.; Chen, Y. P.; Horng, R. H. High-performance transparent barrier films of SiO_x/SiN_x stacks on flexible polymer substrates. *J. Electrochem. Soc.* **2006**, *153*, F244.

(24) Graff., G. L.; Williford, R. E.; Burrows, P. E. Mechanisms of vapor permeation through multilayer barrier films: Lag time versus equilibrium permeation. *J. Appl. Phys.* **2004**, *96*, 1840.

(25) Kim, D. W.; Choi, H.; Lee, C.; Blumstein, A.; Kang, Y. Investigation on methanol permeability of Nafion modified by self-assembled clay−nanocomposite multilayers. *Electrochim. Acta* **2004**, *50*, 659−662.